

Fail-Safe Generative Adversarial Imitation Learning

Philipp Geiger¹ Christoph-Nikolas Straehle¹

Abstract

For flexible yet safe imitation learning (IL), we propose a modular approach that uses a generative imitator policy with a safety layer, has an overall explicit density/gradient, can therefore be end-to-end trained using generative adversarial IL (GAIL), and comes with theoretical worst-case safety/robustness guarantees. The safety layer’s exact density comes from using a countable non-injective gluing of piecewise differentiable injections and the change-of-variables formula. The safe set (into which the safety layer maps) is inferred by sampling actions and their potential future fail-safe fallback continuations, together with Lipschitz continuity and convexity arguments. We also provide theoretical bounds showing the advantage of using the safety layer already during training (imitation error linear in the horizon) compared to only using it at test time (quadratic error). In an experiment on challenging real-world driver interaction data, we empirically demonstrate tractability, safety and imitation performance of our approach.

1. Introduction and Related Work

For several problems at the current forefront of agent learning, such as control of self-driving vehicles or robots, or modeling/simulation of realistic agents, imitation learning (IL) is gaining momentum as a method, or as one part in methods (Bansal et al., 2018; Zeng et al., 2019; Bhattacharyya et al., 2019; Xu et al., 2020; Suo et al., 2021; Cao et al., 2020). One main reason – besides realism – is that IL often harnesses cheaply available observational demonstrator data, while reinforcement learning (RL) can be more expensive due to issues with exploration and reward design. But *safety* and *robustness* of IL for such tasks remains a challenge – and is surprisingly unexplored.

¹Bosch Center for Artificial Intelligence, Renningen, Germany.
Correspondence to: <philipp.w.geiger@de.bosch.com>.

(Generative) imitation learning The basic idea of imitation learning is as follows: we are given a set of recordings of the behavior of some *demonstrator* agent, and then we train the *imitator* agent on this data such that it behaves similarly to the demonstrator (Osa et al., 2018). One powerful recent IL method is *generative adversarial imitation learning (GAIL)* (Ho & Ermon, 2016; Song et al., 2018). GAIL’s idea is, on the one hand, to use policy gradient methods borrowed from RL (including, implicitly, a form of *planning*) to generate an imitator behavior that matches the demonstrator’s over whole trajectories. And on the other hand, to measure the “matching”, GAIL uses a *discriminator* as in *generative adversarial networks (GANs)* that seeks to distinguish between demonstrator and imitator distributions. While the neural net and GAN aspects help the flexibility of the method, the RL aspects stir against compounding of errors over roll-out horizons, which other IL methods like *behavior cloning (BC)*, which do not have such planning aspects, suffer from. One recent line of research generalizes classic Gaussian policies to more flexible (incl. multi-modal) conditional *normalizing flows* as imitator policies (Ward et al., 2019; Ma et al., 2020) which nonetheless give exact densities/gradients for training via the *change-of-variables formula*.

Safety and robustness challenges While these are substantial advances in terms of *learning flexibility/capacity*, it remains a challenge to make the methods (1) guaranteeably *safe*, especially for decision making in multi-agent interactions with humans, and (2) *robust*, in the sense of certain generalizations “outside the training data”, e.g., longer simulations than training trajectories. Both is non-trivial, since safety and long-term behavior can heavily be affected already by small learning errors (similar as the *compounding error* of BC).

Safe control/RL frameworks we build on Safe control is commonly formulated as finding controls of a dynamic system that guarantee to keep the system collision-free/safe, over some finite or infinite horizon, under assumptions. Several ideas that are particularly relevant for us are: (1) a formulation in terms of keeping a collision cost function within certain constraints in a restricted worst case dynamics, known from *reachability analysis/games* within control (Fridovich-Keil & Tomlin, 2020; Bansal et al., 2017).

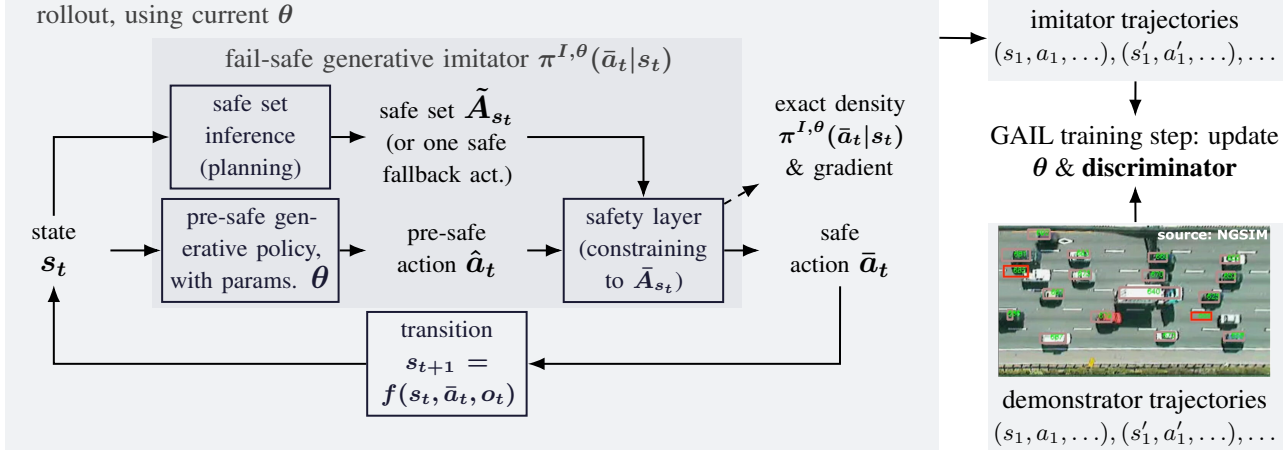


Figure 1: *Left*: our proposed imitator $\pi^{I,\theta}(a|s)$ during a rollout. *Right*: training of the imitator’s parameters θ , based on a discriminator that punishes dis-similarity between imitator’s and demonstrator’s average state/action distributions, i.e., GAIL training. While our method is for general safe IL tasks, we take driver imitation as running example/experiments.

(2) Any learning-based policy can be made safe by, at each stage, constraining its action to a set of “fail-safe actions”, meaning actions for which we know that *at least one subsequent safety controller exists* (Wabersich & Zeilinger, 2018). (3) Often it is enough to search over a reasonably small set of candidates for safety controllers (or “fallback maneuvers”), such as emergency brakes and simple evasive maneuvers in autonomous driving (Pek & Althoff, 2020). And (4) an easy way to constrain a policy’s output to such safe actions is by concatenating it with a *safety layer* that maps into the constrained set, and *differentiable* safety layers can even be used during *training* (Donti et al., 2021; Dalal et al., 2018).

Safe (generative) IL, theoretical guarantees, and their limitations While incorporating *safety* into *RL* has received significant attention in recent years (Wabersich & Zeilinger, 2018; Berkenkamp et al., 2017; Chow et al., 2019), *safety in IL*, and its *theoretical analysis*, have received comparably little attention.¹ To have a rough classification of the existing safe IL work, a first distinction can be made in terms of safety via *reward augmentation* versus *safety layers/constraints within the policy*. In *reward augmentation*, loss terms are added to the imitation loss (e.g., GAIL loss) that penalizes undesired state-action pairs (e.g., collisions) (Bhattacharyya et al., 2019; 2020; Bansal et al., 2018; Suo et al., 2021; Zeng et al., 2020). Regarding *safety layers and hard-constrained policies*, one line of research is deep IL with safety layers, but *only during test time* (Chen et al., 2019). There is little work that uses safety layers during *train and test time*, with the notable exception of (Yin et al., 2021) (non-generative but with guarantees).

¹One reason may be that IL often does not require exploration, but this is just one mode where safety is a severe issue.

However, we are not aware of any generative IL approaches that have (1) *guaranteed*, tractable, hard-constrained safety, and (2) safety layers already during training, with *closed-form imitator policy density/gradient*, important, in particular, for policy gradient-based training.

Main contributions and paper structure In this paper, we take a basic step towards addressing the mentioned challenges and gaps. We propose the modular methodology *fail-safe generative adversarial imitation learning (FASGAIL*; Sec. 3) illustrated in Fig. 1, consisting of:²³

- a class of tractable *safety layers*, which guaranteeably constrain a given “pre-safe” action into a given safe action set, and consist of countably many non-injectively stuck-together differentiable injections. This allows for the change-of-variables formula to be applied to get *exact densities/gradients* (Prop. 1) – so that it can already be used *during training* (GAIL-based) – while mitigating the rigid injectivity requirements of a pure change-of-variables approach. This layer is concatenated to a generative pre-safe policy, e.g., a Gaussian or, more generally, normalizing flow, that conditions on the state.
- To obtain the current safe set (that the above safety layer needs as input), we propose two types of *safe set inference modules*.⁴ They provably yield safe action sets, in spite of

²Note that our approach works with both, demonstrators that are already fully safe, but also those that may be unsafe.

³Regarding the task of realistic modeling/simulation: Adding safety constraints can, in principle, lead to unrealistic biases in case of unsafe demonstrations. But the other extreme is pure IL where, e.g., collisions rates can be unrealistically high (Bansal et al., 2018). So this is always a trade-off.

⁴Other safety approaches can be plugged in as well.

just checking finitely many actions' safety, using Lipschitz-continuity/extremality arguments (Prop. 2 and 3), mitigating the limitations of purely analytic safety approaches.

Furthermore, regarding additional theory (generally, proofs are in the Appendix A) and experiments:

- A general question is to what extent it helps to use the *safety layer already during training (as we do)*, compared to just concatenating it, at *test* time, to an unsafely trained policy, given the latter may computationally be much easier. We theoretically quantify the imitation performance advantage of the former over the latter: essentially, the former imitation error scales *linearly* in the roll-out horizon, the latter *quadratically* (Sec. 4, rem. 2, and thm. 1) – reminiscent of BC. The intuition: only the former method learns how to properly deal (plan) with the safety layer, while in the latter case, the safety layer may *lead to unvisited states at test time from which we did not learn to recover*.
- In experiments on real-world highway data with multiple interacting driver agents (which also serves as running example throughout the paper), we empirically show tractability and safety (w.r.t. fixed and moving obstacles) of our method, and show that its imitation/prediction performance comes close to unconstrained GAIL baselines (Sec. 5).

2. Setting and Problem Formulation

Setting, definitions and notation We consider episodes of a dynamic system consisting of:

- *states* $s_t \in S$, at *time stages* $t \in 1:T := \{1, \dots, T\}$;
- an *ego agent* that takes *action* $a_t \in A \subset \mathbb{R}^n, n \in \mathbb{N}$, according to its *ego policy* π_t ; we allow π_t to be either a conditional (Lebesgue) density, writing $a_t \sim \pi_t(a|s_t)$, or deterministic, writing $a_t = \pi(s_t)$;
- the ego agent can be either the *demonstrator*, denoted by π^D , or the *imitator*, denoted by $\pi^{I,\theta}$, with θ its parameters;
- *other agents* – also interpretable as *noise/perturbations* in the environment – with their (*joint*) *action* o_t according to *others' policy* φ_t (density/deterministic, analogous to ego);
- the system's *transition function* (environment) f , which we assume to be known, s.t.,

$$s_{t+1} = f(s_t, a_t, o_t), \quad (1)$$

- *imitation cost function* $c(s, a)$, and *safety/collision cost* $d(s)$; states s for which $d(s) \leq 0$ are referred to as *collision-free* or *feasible*;
- notation: τ denote trajectories (s_0, a_0, \dots) , $P(\cdot)$ denotes probability, and $p_x(\cdot)$ the density of x , if it exists.

Problem formulation The goal is for the imitator to generate trajectories that minimize the imitation cost, while satisfying a safety cost constraint, formally:

$$\pi^I = \arg \min_{\pi} \mathbb{E}_{\pi} \left(\sum_{t=1}^T c(s_t, a_t) \right) - \psi(\pi), \quad (2a)$$

$$d(s_t) \leq 0, \text{ for all } t, \quad (2b)$$

where $v^{\pi, c, \psi}$ is called *imitation value function* (we drop superscript ψ if it is zero), $\psi(\pi)$ is a *policy regularizer*, and $\mathbb{E}_{\pi}(\cdot)$ denotes the expectation over roll-outs of π .⁵⁶

We purportedly stay fairly abstract here. We will later show how the imitation loss c can formalize the similarity between imitator and demonstrator (via the GAIL loss in Sec. 3.3), and specify ψ (Sec. 3.3) and d (Sec. 5). Furthermore, we left the problem underspecified regarding the other agents' behavior/noise, since we want this to depend on the specific safety reasoning, e.g., ours in Sec. 3.2.

3. Method FASGAIL alongside Analysis

In this section, we describe our methodology and part of the theoretical foundations. First, our method consists of the *fail-safe (generative) imitator* $\pi^{I,\theta}(a|s)$. Its structure is depicted on the l.h.s. of Fig. 1, and contains the following modules: at each roll-out stage t , with state s_t as input,

- the *pre-safe generative policy* (e.g., Gauss) gives a pre-safe action \hat{a}_t (detailed in Sec. 3.1),
- the *safe set inference module* outputs an (inner approximation) of the safe set $\bar{A}_t^{s_t}$ (detailed in Sec. 3.2),
- then, s_t plus the approximate $\bar{A}_t^{s_t}$ are fed into the *safety layer module* (detailed in Sec. 3.1) to obtain the safe action \bar{a}_t plus exact density/gradient of $\pi^{I,\theta}(\bar{a}_t|s_t)$.

For *training* of $\pi^{I,\theta}(a|s)$'s parameters/weights θ , our approach builds on GAIL training (Sec. 3.3).

3.1. Safety Layer & Pre-Safe Generative Policy Module

Background, change of variables, pre-safe policy Remember the classic *change-of-variables formula* (Rudin et al., 1964): If $y = e(x)$ for some injective differentiable function e , and x has density $p_x(x)$, then the implied density of y is $|\det(J_{e^{-1}}(y))|p_x(e^{-1}(y))$.⁷ A *normalizing flow* (Papamakarios et al., 2019) is a generative model with explicit closed-form density. It maps samples of a standard Gaussian through an *easily invertible* injective neural net e .

⁵The $\arg \min$ is well defined under appropriate assumptions regarding compactness of action/policy sets, continuity of c , etc.

⁶We assume an initial (or intermediate) state as given.

⁷ J_e denotes the Jacobian matrix of e .

This means its output samples have a flexible yet explicit density, based on the change-of-variables formula. A *conditional (normalizing) flow* extends this idea by taking an additional input to the neural net, thus being able to model a *conditional density*, of which Gaussian policies can be seen as a (1-layer) special case. We use a closed-form conditional generative model, a *pre-safe generative policy*, such as a Gaussian policy or conditional flow, to map state s to a *pre-safe action* sample $\hat{a} \in A$ with explicit probability density $p_{\hat{a}|s}(\hat{a}|s)$.⁸ Now assume we are given a safe action set $\bar{A} \subset A$ (details follow in Sec. 3.2) and we want to add a safety layer, which maps/constraints our pre-safe policy’s output $\hat{a} \in A$ into \bar{A} – without losing the property of having an exact density. Note that the construction of such safety layers $A \rightarrow \bar{A}$ with exact density/gradient *only* based on change of variables is very limited. This can already be seen from topological properties: if \bar{A} is not simply connected, then no such layer can exist (given A is simply connected; details/definitions are in Appendix B.1).

Proposed class of safety layers These limitations motivate our simple yet flexible approach of using the following type of function as *safety layers*⁹:

Definition 1 (Piecewise diffeomorphism safety layers). *We call a function $g : A \rightarrow \bar{A}$ a piecewise differentiable injection (diffeomorphism), if there exists a countable partition $(A_k)_k$ of A , and differentiable (on the interiors) injections $g_k : A_k \rightarrow \bar{A}$, such that $g|_{A_k} = g_k$.*¹⁰

This type of function allows us to combine change of variables with additivity of measures, to immediately obtain:

Proposition 1 (Explicit density for piecewise diffeomorphism). *If g is a piecewise diffeomorphism, $\bar{a} = g(\hat{a})$ and \hat{a} ’s density is $p_{\hat{a}}(\hat{a})$, then \bar{a} ’s density is*

$$p_{\bar{a}}(\bar{a}) = \sum_{k: \bar{a} \in g_k(A_k)} |\det(J_{g_k^{-1}}(\hat{a}))| p_{\hat{a}}(g_k^{-1}(\bar{a})). \quad (3)$$

Remark 1. *Piecewise diffeomorphic safety layers are versatile: If a given safe set \bar{A} contains at least some area (open set), then we can usually map A into \bar{A} , simply by moving and scaling the unsafe areas into safe ones (details are in Appendix A.1.2).*

Specific simple safety layer instance Whenever A is a box (i.e., a (hyper-)rectangle), we propose the following concrete instance (which we use for the experiments in Sec. 5). The partition $(A_k)_k$ is given by the boxes of a

⁸If A is box-shaped, then the squashing into A works by using appropriate sigmoids for each dimension as final layers.

⁹A simpler solution would be to map all unsafe pre-actions to one safe action, i.e., *one point*, but this would lead to stronger biases and we would lose the property of having an overall density.

¹⁰Usually, parts A_k will be topologically simply connected sets.

regular grid lied into A . Regarding g , we do the following, which we believe introduces a helpful *inductive bias*: (a) On all safe parts k , i.e., $A_k \subset \bar{A}$, g_k is the identity, i.e., we just keep the pre-safe proposal \hat{a} . (b) On all unsafe parts k , g_k is the translation to the rectangle where the unconstrained flow density $p_{\hat{a}}$ has the most mass (approximately). Alternatively, in (b) a probabilistic version can be used where g_k translates to safe part A_ℓ with (approximate) probability proportional to $p_{\hat{a}}$ on A_ℓ (this amounts to a conditioning on the safe set, i.e., a renormalization, if the box size goes to zero).

Now, we can simply concatenate the safety layer with the pre-safe policy. Based on the above, this gives us samples of \bar{a} , analytic density $\pi^{I,\theta}(\bar{a}|s_t)$ (by plugging the density $p_{\hat{a}|s}(\hat{a}|s_t)$ into Prop. 1), and gradient $\nabla_\theta \pi^{I,\theta}(\bar{a}|s_t)$ (in the case of conditional flows as pre-safe policy, use their efficient gradient calculation (Papamakarios et al., 2019) plus Prop. 1) for end-to-end training – once we have inferred the current safe set $\bar{A}_t^{s_t}$, which we now describe.

3.2. Safe Set Inference Module with Guarantees

Background In principle, many safety approaches can be plugged as safety modules into our overall method (Fig. 1). This includes frameworks based on Lyapunov functions, Hamilton-Jacobi type equations (continuous time) (Bansal et al., 2017), or Responsibility-Sensitive Safety (RSS) (Shalev-Shwartz et al., 2017).¹¹ Here we present one approach based on a (restricted) worst-case assumption about noise/other agents, which is a common formulation from reachability analysis/games within control (Fridovich-Keil & Tomlin, 2020; Bansal et al., 2017).

Keep in mind our general setting and dynamics from Sec. 2 (where we left open part of the problem – our reasoning of how the other agents/noise actually behave), and assume for this section, that ego/other policies π, φ range over compact sets Π, Φ of deterministic policies. We define the *safe (action) set* in state s at time t as¹²¹³

$$\bar{A}_t^s := \{a \in A : \text{exists } \pi_{t+1:T}, \text{ s.t. for all } \varphi_{t:T}, t < t' \leq T, \\ d(s_t) \leq 0 \text{ holds, when starting from } (s, a) \text{ at } t\}. \quad (4)$$

We refer to actions in \bar{A}_t^s as *safe actions*. It will be helpful

¹¹A fundamental problem in safe control is the trade-off between being safe (conservative) versus allowing for enough freedom to be able to “move at all”. The former frameworks build on more conservative adversarial/worst-case reasoning. RSS’s idea is to prove safety under the assumption of others sticking to (traffic) *conventions*, and if collisions happen nonetheless, then at least the ego is “not to blame”.

¹²We use the general formulation where policies π_t can depend on t . This allows us to easily treat the case where we directly plan an open-loop action trajectory $a_{1:T}$ simultaneously, by simply $\pi_t(s_t) := a_t$, for all t, s_t .

¹³The corresponding *state* set would be an “invariant safe set” (Bansal et al., 2017).

to characterize \bar{A}_t^s as a so-called *subzero set*. For this, define the (*worst-case*) *total safety cost (to go)* as¹⁴

$$w_t(s, a) := \min_{\pi_{t+1:T}} \max_{\varphi_{t:T}} \max_{t' \in t+1:T} d(s_{t'}), \text{ for all } t. \quad (5)$$

It is easy to see that this implies $\bar{A}_t^s = \{a : w_t(s, a) \leq 0\}$.

Now observe that, crucially, at each stage t , the following holds: an ego policy π_t can be part of a feasible, i.e., safety constraint satisfying, solution of our general problem, Eq. (2), for all allowed $\varphi_{t:T}$, *only if its support lies in \bar{A}_t^s* , for each s (because otherwise there exists no worst-case feasible continuation $\pi_{t+1:T}$, by definition of \bar{A}_t^s).

While in certain limited scenarios, it may be possible to compute the safe action set \bar{A}_t^s *exactly* (Rungger & Tabuada, 2017), this is not the case in general. One way to circumvent this, while nonetheless giving guarantees, is to check $w_t(s, a)$ for just a *finite sample* of a 's. And then conclude on the value of $w_t(s, \cdot)$ on these a 's *neighborhoods*, using Lipschitz continuity¹⁵ or extremality/convexity arguments (Gillula et al., 2014).¹⁶ This at least would give an *inner approximation* \tilde{A}_t^s of the safe set (inner approximation means that, while \tilde{A}_t^s and \bar{A}_t^s may not coincide, we know for sure that $\tilde{A}_t^s \subset \bar{A}_t^s$, i.e., \tilde{A}_t^s is safe).

The following result gives us this Lipschitz continuity and constant.¹⁷ It builds on the simple fact that maximization/minimization preserves Lipschitz continuity (a known fact that lies somewhere between *envelope theorem* and *maximum theorem*).

Proposition 2 (Lipschitz constants for total safety cost). *Assume the momentary safety cost d is α -Lipschitz. Let transition f and policy classes Π, Φ be such that for all (deterministic) ego/other policies $\pi \in \Pi, \varphi \in \Phi$, the dynamics $s \mapsto f(s, \pi(s), \varphi(s))$ and $a \mapsto f(s, a, \varphi(s))$ are β -Lipschitz. Then $a \mapsto w_t(s, a)$ is $\alpha \max\{1, \beta^T\}$ -Lipschitz.*

A second approach to inner-approximate \bar{A}_t^s is based on the notion that sometimes, knowing the safety of a *finite set of corners/extremal points that “span” a set* is enough to know that the full set itself is safe. This can be made rigorous in

¹⁴Note: The minima/maxima are well-defined, once we make appropriate continuity assumptions. A-temporally, this can be seen as a Stackelberg game. The others' maxima may often collapse to open-loop trajectories. The finite horizon can be extended to the infinite case using terminal safety terms (Pek & Althoff, 2020).

¹⁵Lipschitz/continuity understanding is helpful also for other things: e.g., understanding the safe set's topology for Sec. 3.1.

¹⁶Stated differently, we can use *single-action safety checkers* (in the sense of the “*doer-checker*” approach (Koopman et al., 2019)) as oracles for action-set safety inference.

¹⁷We assume all spaces are implicitly equipped with norms. The key conclusion is that, once we know that $w_t(s, \cdot)$ is α -Lipschitz, and that $w_t(s, a) < 0$, then we also know that $w_t(s, \cdot)$ is negative on a ball of radius $\frac{w_t(s, a)}{\alpha}$ around a .

various ways, here we give a version based on convexity.¹⁸

Proposition 3 (Extremality-based safety). *Assume the dynamics f is linear, and the ego/other policy classes Π, Φ consist of open-loop policies, i.e., action trajectories, and that safety cost d is convex.¹⁹ Then $a \mapsto w_t(s_t, a)$ is convex. In particular, for any convex polytope $B \subset A$, $w_t(s, \cdot)$ takes its maximum at one of the (finitely many) corners of B .*

Proposed safe set inference module/algorithm Now we describe our inference of the inner-approximated safe set \tilde{A}_t^s . We partition the action set A into regular boxes (hyperrectangles) $(A_k)_{k=1}^K$, as we already did in Sec. 3. Then, given stage t with state s_t , we simply go over each box A_k and determine its safety by evaluating²⁰ $w_t(s_t, a)$, with

- either a the center of A_k , and then using the Lipschitz continuity argument (Prop. 2) to check if $w_t(s_t, \cdot) \leq 0$ on the full A_k ,
- or a ranging over all corners of box A_k , yielding safety of this box iff $w_t(s_t, \cdot) \leq 0$ on all of them (Prop. 3).

Then, as inner-approximated safe set \tilde{A}_t^s , return the union of all safe boxes A_k . As an important simplification which preserves guarantees, for any t , in the evaluation of $w_t(s_t, a)$, we let the ego policies range over some small, sometimes finite set $\bar{\Pi}_{t+1:T} \subset \Pi_{t+1:T}$ of reasonable *fallback* future continuations of ego policies – i.e., after a_t is taken. In the case of autonomous driving (see experiments), $\bar{\Pi}_{t+1:T}$ consists of *emergency brake* and *evasive maneuvers* (additional details are in Appendix B.2).

Invariant fail-safe fallbacks and guarantees Additionally, to cope with the fact that there may not always be a *fully safe* part A_k (even though an *individual* safe action exists), we propose the following, inspired by (Pek & Althoff, 2020): starting at a presumably safe stage 1, at each stage t , remember *one* fail-safe fallback future ego policy $\pi_{t+1:T}^f$. Then, if no fully safe part A_k (including a new fail-safe fallback) is found anymore at $t+1$, execute the fail-safe fallback π_{t+1}^f , and keep $\pi_{t+2:T}^f$ as new fail-safe fallback (in Appendix B.3.2 we comment on potential training issues with this).²¹ Based on the above, if we know at least one

¹⁸Note that (Gillula et al., 2014) also inner-approximate safe sets from finite samples of the current action space (and then checking the continuation trajectory for safety), by using the convex hull argument. However, Prop. 2 is better tailored to our setting, in particular allowing for other agents.

¹⁹Open-loop is a restriction but note that we do search over *all* trajectories in Π, Φ , so it is similar to trajectory-based planning.

²⁰Clearly, already the “checker” task of evaluating a single action's safety value, Eq. (5), can be non-trivial. But often, roll-outs, analytic steps, convex optimizations or further inner approximations can be used, or combinations of them, see also Sec. 5.

²¹In stable linear systems it can in fact often be guaranteed that always a full safe box is found.

safe action at stage 1, it is easy to see that we can *guarantee* that the ego will be safe throughout the horizon $1:T$.

3.3. Imitation Cost and Training based on GAIL

To specify the imitation loss $c(s, a)$ (which we left abstract in Sec. 2), in principle various frameworks can be applied. We propose to use GAIL (Ho & Ermon, 2016). In GAIL, roughly speaking, $c(s, a)$ is given by a GAN’s *discriminator* value between imitator and demonstrator, because the discriminator (at its optimum) measures the deviation between imitator and demonstrator (average state-action distribution). As policy regularizer $\psi(\pi)$ in Eq. (2), we take π ’s differential entropy. Further details are in Appendix B.3.

Training: As illustrated on the r.h.s. of Fig. 1, analogous to usual GAIL approaches, essentially training consists of steps alternating between: (a) doing roll-outs of our fail-safe imitator $\pi^{I, \theta}(a|s)$ under current parameter θ to sample imitator state-action trajectories (the *generator*), (b) obtain new imitator parameter θ' by optimizing an estimated Eq. (2) from these trajectory samples, using policy gradient approaches (Haarnoja et al., 2018; Sutton & Barto, 2018) for which the exact policy density formula (Prop. 1) and its gradient is crucial, (c) obtain new discriminator parameters based on optimizing an estimate of the discriminator loss, based on trajectory samples of both, imitator π^I and demonstrator π^D (further details are in Appendix B.3).

4. Analysis: Train-&-Test vs. Test-Only Safety

In our method described in Sec. 3, we advocate to use the safety layer already during training. But we could also use it only during test/production time, which would nonetheless be safe, but much easier computationally. The latter is an approach that also other safe IL work takes (Chen et al., 2019), but it means that the test-time policy differs from the trained one. Therefore, here we seek to answer the following question, which we consider relevant for a foundational understanding of safe (GA)IL beyond our specific method:

What is the difference, in terms of imitation performance, between using a safety layer only during test time, compared to using it during training and test time?

The analysis we give in this section is inspired by – and will feel reminiscent of – analysis of the *compounding errors* incurred by behavior cloning (BC) (Ross & Bagnell, 2010; Syed & Schapire, 2010; Xu et al., 2020) (though the setting is somewhat different). Here, let us make the following assumptions and definitions (some familiar from the mentioned BC/IL work):²²

²²We believe that most of the simplifying assumptions we make can be relaxed, but the analysis will be much more involved.

- the state space S and action space A are discrete;
- the *time-averaged state-action distribution* is defined – as usual – as $\rho(s, a) = \left(\frac{1}{T} \sum_{t=1}^T p_{st}(s)\right) \pi(a|s)$, for all s, a ;
- as before, π^D is the demonstrator, π^I the imitator trained with our *train-and-test-time safety layer* approach (Sec. 3). Additionally define π^U as a classic, *unsafe/unconstrained trained imitator* policy²³, π^O as the *test-time-only safety policy* obtained by concatenating π^U with some safety layer at test time. Let $\rho^D, \rho^I, \rho^U, \rho^O$ denote the corresponding state-action distributions.
- As is common (Ross & Bagnell, 2010; Xu et al., 2020), we measure performance deviations in terms of the (unknown) demonstrator cost function, which we denote by c^* (i.e., in the fashion of inverse reinforcement learning (IRL), where the demonstrator is assumed to be an optimizer of Eq. (2a) with c^* as c); and assume c^* only depends on s , and $\|c^*\|_\infty$ is its maximum value. Let $v^D := v^{\pi^D, c^*}$, $v^I := v^{\pi^I, c^*}$, $v^O := v^{\pi^O, c^*}$ be the corresponding imitation value functions (Sec. 2).
- We assume that (1) the demonstrator is fully safe, and (2) the safety layer is the non-identity only on actions that are never taken by the demonstrator (mapping them to safe ones). Importantly, note that *if we relax these assumptions, in particular, allow the demonstrator to be unsafe, the results in this section would get even stronger* (the difference of adding a safety layer would be even bigger).

For the following results, keep in mind: what we can expect to achieve by GAIL training is a population-level closeness of the imitator to the demonstrator distribution of the form $D(\rho^I, \rho^D) \leq \varepsilon$, for some ε decreasing in the sample size, and D , for instance, the Jensen-Shannon distance (due to the usual bias/generalization error). So we make this an assumption in the following results. Note that we use $D = D_{KL}$, the *Kullback-Leibler divergence*, which simplifies parts of the derivation, though we believe that it can be extended.

Now, first, observe that for our “train and test safety layer” approach (Sec. 3), we have a *linear* (in the horizon T) imitation performance guarantee. This is because the *imitator* π^I is explicitly trained to deal with the safety layer (i.e., either to plan to avoid safe but poor states in the first place, or to at least recover from them when they happen):²⁴

Remark 2. *Assume $D_{KL}(\rho^I, \rho^D) \leq \varepsilon$. Then we get*

$$|v^I - v^D| \leq T \|c^*\|_\infty \sqrt{2\varepsilon} \quad (6)$$

(For details see Appendix A.3.1.) In contrast, using test-

²³In our method’s case this means: the pre-safe policy’s, e.g., Gaussian policy’s, output \hat{a} is directly taken as action a .

²⁴The derivation is similar to established infinite-horizon GAIL guarantees (Xu et al., 2020) (explicit derivation in Appendix A.3.1).

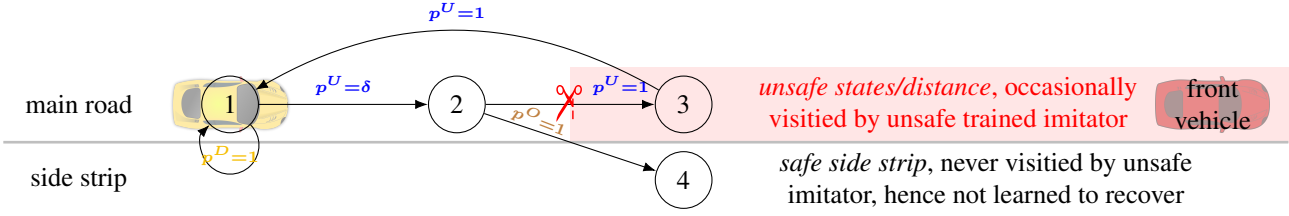


Figure 2: Staying with our running example of driver imitation, this figure illustrates the following: if we use safety layers only at test time and not already during training, the test-time imitator has *not learned to deal with the states that the safety layer may lead to* (i.e. to either plan to avoid, or recover from them), yielding *poor imitation performance*. In a nutshell: The demonstrator is always ($p^D = 1$) in state 1, meaning a constant velocity and distance to the front vehicle. The **unsafely trained imitator** π^U , due to learning error, with low probability $p^U = \delta$, deviates from state 1 and reaches first state 2 and then (due to, say, inertia) unsafe state 3, from which it has learned to always recover though. The **test-safe-only imitator** π^O , like the unsafely trained imitator it builds upon, with low probability $p^O = \delta$ reaches state 2. But from there, the **safety constraints** (**red scissors** symbol) kick in and the only remaining action is to *go to the side strip 4* with $p^O = 1$, where there was *no data on how to recover* (never visited/learned by unsafe π^U), getting trapped there forever. Details are in Appendix A.3.2.

time-only safety, the test-time imitator π^O *has not learned to plan with, and recover from, the states that the safety layer may lead to*, leading to a (tight) quadratic error bound²⁵ (proved in Appendix A.3.2):

Theorem 1 (Quadratic error of test-time-only safety layer). **Lower bound** (an “existence” statement): *There exists an environment²⁶ (with variable horizon T) with a demonstrator, sketched in Fig. 2, with additional details in Appendix A.3.2, some universal constant ι , and, for every $\varepsilon > 0$, an unconstrained imitator π^U with $D_{KL}(\rho^D, \rho^U) \leq \varepsilon$, such that for the induced test-time constrained imitator π^O we have, for all ε, T ,*

$$|v^O - v^D| \geq \iota \min\{\varepsilon T^2, T\} \|c^*\|_\infty. \quad (7)$$

Upper bound (a “for all” statement): *Assume $D_{KL}(\rho^D, \rho^U) \leq \varepsilon$ and assume $\rho^U(s)$ has support wherever $\rho^D(s)$ has. Then:*

$$|v^O - v^D| \leq \sqrt{2 \frac{\varepsilon}{\nu} T^2} \|c^*\|_\infty, \quad (8)$$

where ν is the minimum mass of $\rho^D(s)$ (a marginalized out) within the support of $\rho^D(s)$.

5. Experiments

The goal of the following experiments is to demonstrate tractability of our method, and empirically compare safety as well as imitation/prediction performance to baselines.²⁷

²⁵Observe that the lower bound construction even holds when the demonstrator is always safe.

²⁶In this discrete settings, the environment amounts to a Markov decision process (MDP) (Sutton & Barto, 2018).

²⁷Code will be made available upon publication.

We pick driver imitation from real-world data as a task because it is relevant for both, *control* (of vehicles), as well as *modeling* (e.g., of real “other” traffic participants, for safety validation of self-driving “ego” algorithms (Suo et al., 2021)). Furthermore, its characteristics are quite representative of various challenging safe control tasks, in particular including fixed (road boundary) as well as moving obstacles (other cars). It needs to be emphasized that already each separately, GAIL training (with many hyper-parameters, instability issues, etc.) as well as guaranteeable safety (often hard to make tractable) are challenging, and our method builds on a combination of them. So here the focus is on providing a practical implementation, and demonstrating performance on one challenging real-data task, while an extensive empirical study is left to future work.

Data set, preprocessing: We use the open *highD* data set (Krajewski et al., 2018), which consists of 2-D car trajectories (each ~ 20 s) recorded by drones flying over highway sections (we select a straight section with ~ 1500 trajectories). It is increasingly used for benchmarking (Rudenko et al., 2019; Zhang et al., 2020). We filter out other vehicles in a roll-out once they are behind the ego vehicle. This is substantial filtering, but is, in one way or another, commonly done (Pek & Althoff, 2020; Shalev-Shwartz et al., 2017), based on the idea that the ego is not blamable for other cars crashing into it from behind (and otherwise safety may become too conservative; most initial states could already be unsafe if we consider adversarial rear vehicles that deliberately crash from behind). Additionally, we filter out initially unsafe states (using the same filter for all methods). **Setting, simulation:** We do an open-loop simulation where we just replace the ego vehicle by the our method/the baselines, while keeping the others’ trajectories from the original data. As simulation environment, we take

Table 1: Outcome of imitation on real-world driver data, in terms of safety and imitation performance.

Metric	FASGAIL-E (ours)	...-L (ours)	RAIL	GAIL	TTOS
Safety performance: collision probability overall	0.00	0.00	0.15	0.16	0.00
Safety performance: collision prob. with moving obstacles	0.00	0.00	0.04	0.05	0.00
Imitation/prediction performance: MAE	0.96	0.96	0.69	0.72	1.4
Imitation/prediction performance: RMSE	1.12	1.11	0.75	0.78	1.71

a simple double integrator dynamics as f (on 2-D action space). As collision/safety cost $d(s_t)$, we take minus the minimum l_∞ distance of ego to other vehicles (axis-aligned bounding boxes) and road boundary (it is particularly easy to compute), which is 1-Lipschitz w.r.t. itself/|·|.

Policy fail-safe imitator (FASGAIL-E, -L): We use a Gaussian as pre-safe policy, but also consider a normalizing flow. As safety layer we use the box-based, approximate conditioning instance described in Sec. 3.1. As learnable state feature we use a common image-based feature that abstractly depicts other agents and road boundary fed into a convolutional nets (CNNs) for dimensionality reduction, similar as described in (Chai et al., 2019). Details are in Appendix B.4. *Safe set inference module:* In this double integrator setting, the others’ reachable rectangles can directly be computed exactly. To compute action boxes’, A_k ’s, safety, we use both of our proposed approached from Sec. 3.2, *Lipschitz-based (FASGAIL-L)* and *extremality-based (-E)* building on Prop. 2 and 3 respectively. (Note that strictly, only the conditions of Prop. 2 are met by the setting, however, we believe that also Prop. 3 can be generalized appropriately). As as fail-safe fallback candidates, we use non-linear controllers to generate emergency brake and evasive maneuvers (Pek & Althoff, 2020). **Training:** Training happens with soft actor-critic (SAC) (Kostrikov et al., 2018; Haarnoja et al., 2018) as policy-gradient-based training (part (b) in Sec. 3.3), based on our closed-form density/gradient from Sec. 3.1. Further details are in Appendix B.4.

Evaluation, baselines, metrics Baselines are: *reward-augmented generative adversarial imitation learning (RAIL)* (closest comparison from our method class of safe generative IL, discussed in Sec. 1) (Bhattacharyya et al., 2020; 2019), *test-time-only safety (TTOS)* from Sec. 4, and classic *GAIL* (Ho & Ermon, 2016). We evaluate, on the test set, number of collisions over complete roll-outs (including collisions with other vehicles and off-road collisions) as *safety performance* measure; and rooted mean squared error (RMSE) and mean absolute error (MAE) over trajectories of 4s length as *imitation/prediction performance* measure. Further details are in Appendix B.4.

Outcome/discussion The outcome is in Table 1. It empirically validates our theoretical safety claim by reaching 0%

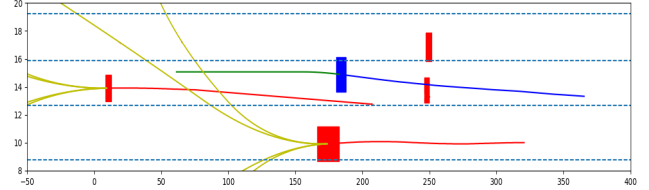


Figure 3: Our trained fail-safe imitator (blue) with its trajectory and future fail-safe fallback emergency brake (green); other vehicles (red), with worst-case reachable boundaries indicated in yellow (rear vehicles are ignored as described).

collisions of our methods (with fixed and moving obstacles). At the same time we come close in prediction performance to the baselines RAIL/GAIL, which, even if using reward augmentation to penalize collisions (RAIL), have significant collision rates. (The rather high collision rate of RAIL may also be due to the comparably small data set we use.) The poorer imitation performance of test-time-only safety layers (TTOS) compared to ours can be read as an empirical average-case confirmation of our theoretical worst-case analysis (Thm. 1). Fig. 3 gives one roll-out sample, incl. ego’s fail-safe and others’ reachable futures considered by our safe set inference. We also experimented with the more expressive case of conditional normalizing flows as pre-safe policy, but they compared unfavorably with Gaussian policies, probably also due to the rather small data regime.

6. Conclusion

In this paper, we took a basic step towards addressing the problem of guaranteeably safe and robust generative imitation learning. We proposed a modular methodology that combines the *flexibility* – i.e., capacity for learning with little hand-crafting – of neural net-based probabilistic policies with *theoretical worst-case safety guarantees*, while maintaining end-to-end generative trainability using our piecewise diffeomorphic safety layer. In first experiments on real-world driver data we demonstrated tractability, safety and imitation performance. The flexibility of our approach is key for realistic, multi-modal modeling but may also help control tasks in the sense of uncertainty quantification and mixed (adversarial) strategies. While safety is directly rel-

event for control tasks, it can also serve as an inductive bias for modeling tasks. And our method’s closed-form densities/gradients are relevant for training in both tasks.

Acknowledgements We thank Mathias Buerger, Maxim Dolgov, Christian Heinemann, Malte Kuhlmann and Felix Schmitt for helpful discussions.

References

Adam, L., Horčík, R., Kasl, T., and Kroupa, T. Double oracle algorithm for computing equilibria in continuous games. *Proc. of AAAI-21*, 2021.

Amos, B. and Kolter, J. Z. Optnet: Differentiable optimization as a layer in neural networks. In *Proceedings of the 34th International Conference on Machine Learning-Volume 70*, pp. 136–145. JMLR. org, 2017.

Amos, B., Jimenez, I., Sacks, J., Boots, B., and Kolter, J. Z. Differentiable mpc for end-to-end planning and control. In *Advances in Neural Information Processing Systems*, pp. 8289–8300, 2018.

Bai, S., Kolter, J. Z., and Koltun, V. Deep equilibrium models. In *Advances in Neural Information Processing Systems*, pp. 688–699, 2019.

Bansal, M., Krizhevsky, A., and Ogale, A. Chauffeurnet: Learning to drive by imitating the best and synthesizing the worst. *arXiv preprint arXiv:1812.03079*, 2018.

Bansal, S., Chen, M., Herbert, S., and Tomlin, C. J. Hamilton-jacobi reachability: A brief overview and recent advances. In *2017 IEEE 56th Annual Conference on Decision and Control (CDC)*, pp. 2242–2253. IEEE, 2017.

Berkenkamp, F., Turchetta, M., Schoellig, A. P., and Krause, A. Safe model-based reinforcement learning with stability guarantees. *arXiv preprint arXiv:1705.08551*, 2017.

Besserve, M. and Schölkopf, B. Learning soft interventions in complex equilibrium systems. *arXiv preprint arXiv:2112.05729*, 2021.

Bhattacharyya, R., Wulfe, B., Phillips, D., Kuefler, A., Morton, J., Senanayake, R., and Kochenderfer, M. Modeling human driving behavior through generative adversarial imitation learning. *arXiv preprint arXiv:2006.06412*, 2020.

Bhattacharyya, R. P., Phillips, D. J., Liu, C., Gupta, J. K., Driggs-Campbell, K., and Kochenderfer, M. J. Simulating emergent properties of human driving behavior using multi-agent reward augmented imitation learning. In *2019 International Conference on Robotics and Automation (ICRA)*, pp. 789–795. IEEE, 2019.

Boborzi, D., Kleinicke, F., Buchner, J., and Mikelsons, L. Learning to drive from observations while staying safe. 2021. upcoming.

Cao, Z., Büyükköse, E., Wang, W. Z., Raventos, A., Gaidon, A., Rosman, G., and Sadigh, D. Reinforcement learning based control of imitative policies for near-accident driving. *arXiv preprint arXiv:2007.00178*, 2020.

Caputo, M. R. The envelope theorem and comparative statics of nash equilibria. *Games and Economic Behavior*, 13(2):201–224, 1996.

Chai, Y., Sapp, B., Bansal, M., and Anguelov, D. Multipath: Multiple probabilistic anchor trajectory hypotheses for behavior prediction. *arXiv preprint arXiv:1910.05449*, 2019.

Chen, J., Yuan, B., and Tomizuka, M. Deep imitation learning for autonomous driving in generic urban scenarios with enhanced safety. *arXiv preprint arXiv:1903.00640*, 2019.

Chow, Y., Nachum, O., Faust, A., Duenez-Guzman, E., and Ghavamzadeh, M. Lyapunov-based safe policy optimization for continuous control. *arXiv preprint arXiv:1901.10031*, 2019.

Dalal, G., Dvijotham, K., Vecerik, M., Hester, T., Paduraru, C., and Tassa, Y. Safe exploration in continuous action spaces. *arXiv preprint arXiv:1801.08757*, 2018.

Donti, P. L., Roderick, M., Fazlyab, M., and Kolter, J. Z. Enforcing robust control guarantees within neural network policies. In *International Conference on Learning Representations*, 2021.

El Ghaoui, L., Gu, F., Travacca, B., and Askari, A. Implicit deep learning. *arXiv preprint arXiv:1908.06315*, 2019.

Fridovich-Keil, D. and Tomlin, C. J. Approximate solutions to a class of reachability games. *arXiv preprint arXiv:2011.00601*, 2020.

Geiger, P. and Straehle, C.-N. Learning game-theoretic models of multiagent trajectories using implicit layers. In *Proceedings of the AAAI Conference on Artificial Intelligence*, volume 35, pp. 4950–4958, 2021.

Gillula, J. H., Kaynama, S., and Tomlin, C. J. Sampling-based approximation of the viability kernel for high-dimensional linear sampled-data systems. In *Proceedings of the 17th international conference on Hybrid systems: computation and control*, pp. 173–182, 2014.

Haarnoja, T., Zhou, A., Abbeel, P., and Levine, S. Soft actor-critic: Off-policy maximum entropy deep reinforcement learning with a stochastic actor. In *International*

conference on machine learning, pp. 1861–1870. PMLR, 2018.

Ho, J. and Ermon, S. Generative adversarial imitation learning. *Advances in neural information processing systems*, 29:4565–4573, 2016.

Huang, J., Xie, S., Sun, J., Ma, Q., Liu, C., Shi, J., Lin, D., and Zhou, B. Learning a decision module by imitating driver’s control behaviors. *arXiv preprint arXiv:1912.00191*, 2019.

Koopman, P., Kane, A., and Black, J. Credible autonomy safety argumentation. In *27th Safety-Critical Systems Symposium*, 2019.

Kostrikov, I., Agrawal, K. K., Dwibedi, D., Levine, S., and Tompson, J. Discriminator-actor-critic: Addressing sample inefficiency and reward bias in adversarial imitation learning. *arXiv preprint arXiv:1809.02925*, 2018.

Krajewski, R., Bock, J., Kloeker, L., and Eckstein, L. The highD Dataset: A Drone Dataset of Naturalistic Vehicle Trajectories on German Highways for Validation of Highly Automated Driving Systems. In *2018 IEEE 21st International Conference on Intelligent Transportation Systems (ITSC)*, 2018.

Lanctot, M., Zambaldi, V., Gruslys, A., Lazaridou, A., Tuyls, K., Pérolat, J., Silver, D., and Graepel, T. A unified game-theoretic approach to multiagent reinforcement learning. *arXiv preprint arXiv:1711.00832*, 2017.

Ling, C. K., Fang, F., and Kolter, J. Z. What game are we playing? End-to-end learning in normal and extensive form games. In *IJCAI-ECAI-18: The 27th International Joint Conference on Artificial Intelligence and the 23rd European Conference on Artificial Intelligence*, 2018.

Ling, C. K., Fang, F., and Kolter, J. Z. Large scale learning of agent rationality in two-player zero-sum games. In *Proceedings of the AAAI Conference on Artificial Intelligence*, volume 33, pp. 6104–6111, 2019.

Luteberget, B. S. Numerical approximation of conformal mappings. Master’s thesis, Institutt for matematiske fag, 2010.

Ma, X., Gupta, J. K., and Kochenderfer, M. J. Normalizing flow policies for multi-agent systems. In *International Conference on Decision and Game Theory for Security*, pp. 277–296. Springer, 2020.

Osa, T., Pajarinen, J., Neumann, G., Bagnell, J. A., Abbeel, P., and Peters, J. An algorithmic perspective on imitation learning. *arXiv preprint arXiv:1811.06711*, 2018.

Otto, F., Becker, P., Vien, N. A., Ziesche, H. C., and Neumann, G. Differentiable trust region layers for deep reinforcement learning. *arXiv preprint arXiv:2101.09207*, 2021.

Paden, B., Čáp, M., Yong, S. Z., Yershov, D., and Frazzoli, E. A survey of motion planning and control techniques for self-driving urban vehicles. *IEEE Transactions on intelligent vehicles*, 1(1):33–55, 2016.

Papamakarios, G., Nalisnick, E., Rezende, D. J., Mohamed, S., and Lakshminarayanan, B. Normalizing flows for probabilistic modeling and inference. *arXiv preprint arXiv:1912.02762*, 2019.

Pek, C. and Althoff, M. Fail-safe motion planning for online verification of autonomous vehicles using convex optimization. *IEEE Transactions on Robotics*, 37(3):798–814, 2020.

Ross, S. and Bagnell, D. Efficient reductions for imitation learning. In *Proceedings of the thirteenth international conference on artificial intelligence and statistics*, pp. 661–668. JMLR Workshop and Conference Proceedings, 2010.

Rudenko, A., Palmieri, L., Herman, M., Kitani, K. M., Gavrila, D. M., and Arras, K. O. Human motion trajectory prediction: A survey. *arXiv preprint arXiv:1905.06113*, 2019.

Rudin, W. et al. *Principles of mathematical analysis*, volume 3. McGraw-hill New York, 1964.

Rungger, M. and Tabuada, P. Computing robust controlled invariant sets of linear systems. *IEEE Transactions on Automatic Control*, 62(7):3665–3670, 2017.

Shalev-Shwartz, S., Shammah, S., and Shashua, A. On a formal model of safe and scalable self-driving cars. *arXiv preprint arXiv:1708.06374*, 2017.

Song, J., Ren, H., Sadigh, D., and Ermon, S. Multi-agent generative adversarial imitation learning. *arXiv preprint arXiv:1807.09936*, 2018.

Suo, S., Regalado, S., Casas, S., and Urtasun, R. Trafficsim: Learning to simulate realistic multi-agent behaviors. *arXiv preprint arXiv:2101.06557*, 2021.

Sutton, R. S. and Barto, A. G. *Reinforcement learning: An introduction*. MIT press, 2018.

Syed, U. and Schapire, R. E. A reduction from apprenticeship learning to classification. *Advances in neural information processing systems*, 23:2253–2261, 2010.

Wabersich, K. P. and Zeilinger, M. N. Linear model predictive safety certification for learning-based control. In *2018 IEEE Conference on Decision and Control (CDC)*, pp. 7130–7135. IEEE, 2018.

Ward, P. N., Smofsky, A., and Bose, A. J. Improving exploration in soft-actor-critic with normalizing flows policies. *arXiv preprint arXiv:1906.02771*, 2019.

Xiao, H., Herman, M., Wagner, J., Ziesche, S., Etesami, J., and Linh, T. H. Wasserstein adversarial imitation learning. *arXiv preprint arXiv:1906.08113*, 2019.

Xu, T., Li, Z., and Yu, Y. Error bounds of imitating policies and environments. *arXiv preprint arXiv:2010.11876*, 2020.

Yin, H., Seiler, P., Jin, M., and Arcak, M. Imitation learning with stability and safety guarantees. *IEEE Control Systems Letters*, 2021.

Zeng, W., Luo, W., Suo, S., Sadat, A., Yang, B., Casas, S., and Urtasun, R. End-to-end interpretable neural motion planner. In *Proceedings of the IEEE/CVF Conference on Computer Vision and Pattern Recognition*, pp. 8660–8669, 2019.

Zeng, W., Wang, S., Liao, R., Chen, Y., Yang, B., and Urtasun, R. Dsnet: Deep structured self-driving network. In *European Conference on Computer Vision*, pp. 156–172. Springer, 2020.

Zhang, C., Zhu, J., Wang, W., and Xi, J. Spatiotemporal learning of multivehicle interaction patterns in lane-change scenarios. *arXiv preprint arXiv:2003.00759*, 2020.

Appendix

A. Proofs and remarks

A.1. Proof for Sec. 3

A.1.1. PROP. 1

Proof for Prop. 1. Intuitively it is clear that the results directly follows from combining σ -additivity of measures with the change-of-variables formula. Nonetheless we give a rigorous derivation here.

Keep in mind the following explicit specifications that were left implicit in the main part: In the main part we just stated to assume Lebesgue densities on $A \subset \mathbb{R}^n$, implicitly we assume \mathbb{R}^n with the usual Lebesgue σ -algebra as underlying measurable space, and that all parts are measurable. Furthermore, to be precise, we assume differentiability of the g_k on the *interior* of their respective domain.

Recall that $(A_k)_k$ is a partition of A , and we assumed differentiable injections $g_k : A_k \rightarrow \bar{A}$ (differentiable on $\text{int}(A_k)$ ²⁸), and that such that $g|_{A_k} = g_k$. Let B_k denote the co-domain of g_k , and $B = \bigcup_k B_k$.

Note that based on our assumptions, either g is already measurable, or, otherwise, we can turn it into a measurable function by just modifying it on a Lebesgue null set (the boundaries of the A_k), not affecting the below argument.

Now let P_A denote the original measure on A , and P_B the push-forward measure on $B \subset \bar{A}$ induced by g .

For any measurable set $M \subset B \subset \bar{A}$, we have (based on disjoints)

$$P_B(M) = P_B(M \cap (\bigcup_k B_k \cup (\bar{A} \setminus B))) = P_B(M \cap (\bigcup_k B_k)) = P_B(\bigcup_k M \cap B_k) = \sum_k P_{B_k}(M \cap B_k) \quad (9)$$

with P_{B_k} denoting the restriction of the original measure to B_k . Now, for each k , the change-of-variables formula tells us that on $\text{int}(g_k(\bar{A}_k))$, P_{B_k} has a density, which we refer to as p_a , i.e., $P_{B_k}(M \cap B_k) = \int_M p_a(a) da$, and that it is given by

$$p_a(a) = \sum_{k: a \in \bar{A}_k} |\det(J_{g_k^{-1}}(\hat{a}))| p_{\hat{a}}(g_k^{-1}(a)), \quad (10)$$

and the rest, besides $\text{int}(g_k(\bar{A}_k))$, can be ignored since it is a null set.

□

A.1.2. REM. 1

Elaboration of Rem. 1. Assume the safe set \bar{A} is given as the subzero set of some continuous function $h : A \rightarrow \mathbb{R}$, i.e., $\bar{A} = h^{-1}((-\infty, 0])$, which is the case, e.g., under Prop. 2 below, and that it contains at least some open set. Let B be some (any) ball in this open set.

Here is the simplest construction: Just take $A_1 := h^{-1}((-\infty, 0])$ and $A_2 := h^{-1}((0, \infty))$. Let g_1 (on A_1) be the identity. And let g_2 (on A_2) be a shrinking, such that A_2 has less diameter than B , and a subsequent translation of A_2 into B .

Another construction, which has a better “topological” bias in that it tries to map unsafe parts into *nearby* safe parts works as follows:

If \bar{A} is the subzero set of a continuous function, then the unsafe set is open. So it can be written as the union of its connected components, and each connected component is also open. Therefore, in each connected component k , there is at least one rational number (or, in higher dimensions, the analogous element of \mathbb{Q}^n), so there are at most countably many of them.

So define g_k with domain the component k , and simply being a translation and scaling that moves this component k into a *nearby* open part of the safe set (this is where it becomes more appealing in terms “topological” bias), or, as a default, into B .

Let g be defined by the “union” of these g_k , and on the rest of A , i.e., on the safe set \bar{A} , let it simply be the identity.

□

²⁸ $\text{int}(\cdot)$ is the interior.

A.2. Proofs for Sec. 3.2

A.2.1. PROP. 2

We will need the following well-known result:

Fact 1. *Assume a function $h(x, y)$ is Lipschitz in x with constant L uniformly in y . Then the function $x \mapsto \max_y h(x, y)$ (assuming maxima always exist) is also L -Lipschitz.*

For the sake of completeness, we provide a proof of Fact 1:

Proof of Fact 1. Let $e(x) := \arg \max_y h(x, y)$.

Consider x, x' and let, w.l.o.g., $\max_y h(x, y) \geq \max_y h(x', y)$. Then:

$$|\max_y h(x, y) - \max_y h(x', y)| = \max_y h(x, y) - \max_y h(x', y) \quad (11)$$

$$= h(x, e(x)) - h(x', e(x')) \quad (12)$$

$$\leq h(x, e(x)) - h(x', e(x)) \quad (13)$$

$$\leq L\|x - x'\|. \quad (14)$$

(We showed the statement for the case that a supremum is always taken, i.e., is a maximum. For the supremum version we refer the reader to related work.²⁹)

□

Now to the proof itself:

Proof for Prop. 2. The idea is to first propagate the Lipschitz continuity through the dynamics, and then iteratively apply Fact 1 to the min/max operations.

Here, for any Lipschitz continuous function e , let L_e denote its constant. Furthermore, we may write π, φ as shorthand for $\pi_{t:T}, \varphi_{t:T}, t \in 1 : T$, respectively.

First observe the following, given an arbitrary but fixed t and π, φ :

Let

$$g(s, \pi, \varphi) := f(s, \pi(s), \varphi(s)) \quad (15)$$

and $h(s, \pi, \varphi, k)$ be defined as the k -times concatenation of $g(\cdot, \pi, \varphi)$, i.e., a roll out; and then define function i by also including the initial action, i.e., and

$$i(s, a, \pi, \varphi, k) := h(f(s, a, \varphi(s)), \pi, \varphi, k). \quad (16)$$

Then, by our assumptions, for π, φ, k arbitrary but fixed,

$$s \mapsto d(h(s, \pi, \varphi, k)) \quad (17)$$

is Lipschitz continuous in s with constant (uniformly in π, φ, k)

$$L_d L_{f(\cdot, \pi(\cdot), \varphi(\cdot))}^k = \alpha \beta^k, \quad (18)$$

since it is the concatenation of d , which is α -Lipschitz, with the k -times concatenation of g , which is β -Lipschitz by assumption. This together with our assumption implies that, for any arbitrary but fixed s , also

$$a \mapsto d(i(s, a, \pi, \varphi, k)) (= w_t(s, a)) \quad (19)$$

²⁹For a proof, see e.g., <https://math.stackexchange.com/questions/2532116/max-operator-over-a-lipschitz-function-is-still-lipschitz>.

is Lipschitz with constant (for any k)

$$\alpha\beta^k\beta = \alpha\beta^{k+1} \leq \alpha \max\{1, \beta^T\}. \quad (20)$$

Now let s be arbitrary but fixed. Also let π be arbitrary but fixed. Then, based on the above together with Fact 1,

$$a \mapsto \max_{\varphi_{t:T}} \max_{t \in t+1:T} d(i(s, a, \pi, \varphi, t)) (=: e(a, \pi)) \quad (21)$$

is Lipschitz with constant $\alpha \max\{1, \beta^T\}$. Again applying Fact 1, we see that also

$$a \mapsto \min_{\pi_{t+1:T}} \max_{\varphi_{t:T}} \max_{t \in t+1:T} d(i(s, a, \pi, \varphi, t)) (= \min_{\pi_{t+1:T}} e(a, \pi)) \quad (22)$$

is Lipschitz with constant $\alpha \max\{1, \beta^T\}$. \square

Remark 3. Alternative versions of this result could be based, e.g., on the “Envelope Theorem for Nash Equilibria” (Caputo, 1996).

A.2.2. PROP. 3

*Proof for Prop. 3.*³⁰

Let the mapping i be defined as in Eq. (16). Fix s .

Observe that, based on our linearity/convexity assumptions, for any φ, t fixed,

$$d(i(s, a, \pi, \varphi, t)) \quad (23)$$

is convex as a function of a, π . But then (because the element-wise maximum over a family of convex functions is also convex) also the maximum over φ, t , i.e.,

$$\max_{\varphi_{t:T}} \max_{t \in t+1:T} d(i(s, a, \pi, \varphi, t)) \quad (24)$$

is convex.

One step further, this means (since convexity is preserved by “minimizing out one variable over a convex domain”) that also taking the minimum over π preserves convexity, i.e.,

$$w_t(s, a) = \min_{\pi_{t+1:T}} \max_{\varphi_{t:T}} \max_{t \in t+1:T} d(i(s, a, \pi, \varphi, t)) \quad (25)$$

is convex as a function of a .

But a convex function over a (compact) convex set that is spanned by a set of corners, takes its maximum at (at least one) of the corners. \square

A.3. Proofs and precise counterexample figure/MDP/agents for Sec. 4

In this section, if not stated otherwise, $\|\cdot\|$ refers to the l_1 -norm $\|\cdot\|_1$.

Keep in mind that, as in the main part, D, I, U, O stand for demonstrator, imitator (our fail-safe imitator with safety layer already during training time), unsafe/unconstrained trained imitator, and test-time-only-safety imitator; and P^D etc. denote the probabilities under the respective policies.

³⁰Proof uses https://en.wikipedia.org/wiki/Convex_function#Operations_that_preserve_convexity

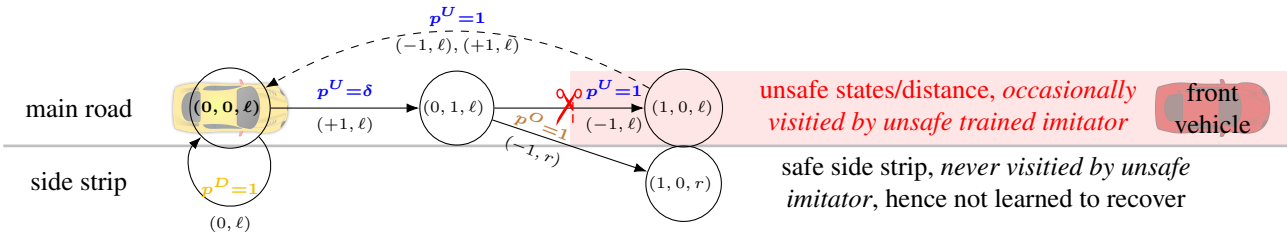


Figure 4: More detailed (but isomorphic) version of the example MDP/agents as in Fig. 2.

A.3.1. REM. 2

We have:

$$\|v^I - v^D\| \quad (26)$$

$$= \left\| \sum_t P_{st}^I c - \sum_t P_{st}^D c \right\| \quad (27)$$

$$= \|cT\left(\sum_t \frac{1}{T} P_{st}^I - \sum_t \frac{1}{T} P_{st}^D\right)\| \quad (28)$$

$$= T \|c(\rho_{st}^I - \rho_{st}^D)\| \quad (\text{Definition } \rho) \quad (29)$$

$$\leq T \|c\|_\infty \|(\rho_{s_t}^I - \rho_{s_t}^D)\| \quad (30)$$

$$\leq T \|c\|_\infty \sqrt{2D_{\text{KL}}(\rho_{s_t, a_t}^{\text{I}}, \rho_{s_t, a_t}^{\text{D}})} \quad (\text{Pinsker's inequality plus marginalization}). \quad (31)$$

A.3.2. THM. 1

Elaboration of the example for the lower bound (Fig. 2) Here, let us first give a precise version – Fig. 4 – of the example in Fig. 2, that is used to get the lower bound in Thm. 1. Instead of the exact Fig. 2, we give an isomorphic version with more detailed/realistic states and actions in terms of relative position/velocity/acceleration/lane.

The Markov decision process (MDP) and agents (policies) are as follows:

MDP: States: The states (of the ego) are triplets $(\delta x, \delta v, \text{lane})$, where δx is deviation from (safe) demonstrator position, δv is deviation from (safe) demonstrator velocity, lane is lane (top or bottom). There are five possible states, all depicted in the figure, except for $(1, -1, \ell)$, to keep the figure instructive. **Actions:** The possible actions are depicted as arrows, with the action $(\text{acc}, \text{lane})$ written below the arrow, where acc means the longitudinal acceleration, and lane the target lane. **Transition:** The longitudinal transition is the usual double integrator of adding acc to δv , while, lateral-wise, lane instantaneously sets the new lane (more realistic but complex examples are possible of course). **Costs:** The true demonstrator's cost c^* is 0 on the demonstrator state $(0, 0, \ell)$, and 1 on every other state.

Agents: *Demonstrator:* Yellow car, always ($p^D = 1$) staying at the depicted position, at a more than safe distance to front car (red). *Unconstrained trained imitator (blue):* due to a slight imitation error ($p^U = \delta$), it is sometimes accelerating, and if it accelerates twice, it reaches an unsafe state, but, as implied by the GAIL loss, always recovers (dashed arrows) back to true demonstrator state. *Safety-constrained test-time imitator (same, except for last action in brown):* as the unconstrained imitator, occasionally ($p^O = \delta$) ends up at rightmost safe state, and then the only remaining safe action is to change lane to the side strip, where there was no data on how to recover, so potentially getting trapped there forever

Proof (remaining) of Thm. 1

Proof for Thm. 1. Lower bound part:

Keep in mind the counterexample construction above. Let s^D denote the state that the demonstrator is constantly in.

Note that the unconstrained imitator in fact satisfies GAIL KL loss:

It is easy to see from the construction that the deviation probability δ of the unconstrained imitator from the demonstrator state can be chosen small enough such that $D_{\text{KL}}(\rho^D, \rho^U) \leq \varepsilon$.

*Proof for the constrained imitator quadratic deviation, case $\varepsilon T \leq 1$:*³¹

Consider the case $\varepsilon T \leq 1$.

By Construction, at each stage t , the probability that the test-time constrained imitator π^O is not in the demonstrator state is the combined probability of not deviating from s^D for k times, $k \leq t$, and then deviating once, i.e.,

$$P^O(s_t \neq s^D) = \sum_{k=1}^t \varepsilon(1-\varepsilon)^{k-1} \quad (32)$$

We have

$$(1-\varepsilon)^k \geq (1 - \frac{1}{T})^k \geq (1 - \frac{1}{T})^T = (1 + \frac{-1}{T})^T \xrightarrow{T \rightarrow \infty} e^{-1} \quad (33)$$

where the first inequality holds because we assumed $\varepsilon \leq \frac{1}{T}$ and so $1 - \varepsilon \geq 1 - \frac{1}{T}$, and the second one because always $k \leq T$. But this implies that there is a constant $\kappa > 0$, such that for T large enough,

$$(1-\varepsilon)^k \geq \kappa. \quad (34)$$

Therefore Eq. (32) can be bounded from below by

$$\sum_{k=1}^t \varepsilon \kappa = t \varepsilon \kappa. \quad (35)$$

Now we get, with the cost vector \vec{c} (i.e., the safety cost function c , but making explicit it is a vector since we are in the discrete case) being 0 in the demonstrator state, and $\|\vec{c}\|_\infty$ elsewhere,

$$|v^O - v^D| \quad (36)$$

$$= \left| \sum_t (P_{s_t}^O - P_{s_t}^D) \cdot \vec{c} \right| \quad (37)$$

$$= \left| \sum_t (P^O(s_t \neq s^D) - 0) \|\vec{c}\|_\infty \right| \quad (38)$$

$$\geq \sum_t (t \varepsilon \kappa) \cdot \|\vec{c}\|_\infty \quad (39)$$

$$\geq \varepsilon \kappa \|\vec{c}\|_\infty \sum_t t \quad (40)$$

$$\geq \varepsilon \kappa' \|\vec{c}\|_\infty T^2 \quad (41)$$

for some κ' (that absorbs both, κ and the deviation between T^2 and $\sum_t t$).

Proof for the constrained imitator quadratic deviation, case $\varepsilon T > 1$:

Alternatively to the previous deviation, we can also write $P^O(s_t \neq s^D)$ as the complementary probability of test-time constrained imitator *not* having deviated from the demonstrator state s^D so far, i.e.,

$$P^O(s_t \neq s^D) = (1 - (1 - \varepsilon)^t) \geq (1 - (1 - \frac{1}{T})^t), \quad (42)$$

since in the current case, $\varepsilon T > 1$ and so $\varepsilon > \frac{1}{T}$ and so $1 - \varepsilon < 1 - \frac{1}{T}$ and so $(1 - \varepsilon)^t < (1 - \frac{1}{T})^t$ and so $1 - (1 - \varepsilon)^t > 1 - (1 - \frac{1}{T})^t$.

³¹Note that this is reminiscent of behavior cloning error analysis (Ross & Bagnell, 2010; Syed & Schapire, 2010), but the construction and proof are different, since we don't need one separate starting state.

Now, for $t \geq \frac{T}{2}$, we get,

$$(1 - \frac{1}{T})^t \leq (1 - \frac{1}{T})^{\frac{T}{2}} = ((1 + \frac{-1}{T})^T)^{\frac{1}{2}} \rightarrow (e^{-1})^{\frac{1}{2}}. \quad (43)$$

Therefore $(1 - \frac{1}{T})^t$ is below and bounded away from 1 for T large enough, and therefore Eq. (42) is bounded away (from above) from 0, i.e., $P^C(s_t \neq s^D)$ is greater $\kappa'' > 0$ for such T large enough and $t \geq \frac{T}{2}$.

Then

$$|v^O - v^D| \quad (44)$$

$$= \left| \sum_{t=1}^T (P_{s_t}^O - P_{s_t}^D) \cdot \vec{c} \right| \quad (45)$$

$$= \left| \sum_{t=1}^T (P^O(s_t \neq s^D) - 0) \|\vec{c}\|_\infty \right| \quad (46)$$

$$\geq \sum_{t=\frac{T}{2}}^T P^O(s_t \neq s^D) \|\vec{c}\|_\infty \quad (47)$$

$$\geq \sum_{t=\frac{T}{2}}^T \kappa'' \|\vec{c}\|_\infty \quad (48)$$

$$= \frac{T}{2} \kappa'' \|\vec{c}\|_\infty \quad (49)$$

$$= \kappa''' T \|\vec{c}\|_\infty. \quad (50)$$

Upper bound part:

In what follows, P stand for probability vectors/matrices, slightly overriding notation, and $P_{s'|s}$ for the transition probability (corresponding to f plus potential noise).

First observe that generally (here P stand for probability vectors/matrices, slightly overriding notation),

$$\Delta_{t+1} := \|P_{S_{t+1}}^O - P_{S_{t+1}}^D\|_1 \quad (51)$$

$$= \|P_{S'|S}^O P_{S_t}^O - P_{S'|S}^D P_{S_t}^D\|_1 \quad (52)$$

$$= \|P_{S'|S}^O P_{S_t}^O - P_{S'|S}^O P_{S_t}^D + P_{S'|S}^O P_{S_t}^D - P_{S'|S}^D P_{S_t}^D\|_1 \quad (53)$$

$$= \|P_{S'|S}^O (P_{S_t}^O - P_{S_t}^D) + (P_{S'|S}^O - P_{S'|S}^D) P_{S_t}^D\|_1 \quad (54)$$

$$\leq \|P_{S'|S}^O (P_{S_t}^O - P_{S_t}^D)\|_1 + \|(P_{S'|S}^O - P_{S'|S}^D) P_{S_t}^D\|_1 \quad (55)$$

First consider the first term in Eq. (55). We can generally, just since the 1-norm of any stochastic matrix is 1, bound it as follows:

$$\|P_{S'|S}^O (P_{S_t}^O - P_{S_t}^D)\|_1 \quad (56)$$

$$\leq \|P_{S'|S}^O\|_1 \Delta_t = 1 \Delta_t \quad (57)$$

Regarding the second term in Eq. (55), we have the following way to bound it.

Keep in mind the following: Let \bar{S} denote the subset of states where $\rho^D(s)$ has support. Since we assumed a finite state/action set, there is some $\nu > 0$ such that $\rho^D(s)$ is greater or equal ν .

Also keep in mind our assumption $D_{KL}(\rho^D, \rho^U) \leq \varepsilon$.³² These assumptions imply

$$\varepsilon \geq D_{KL}(\rho_{s,a}^D, \rho_{s,a}^U) \quad (58)$$

$$= D_{KL}(\pi_{a|s}^D \rho_s^D, \pi_{a|s}^U \rho_s^U) \quad (59)$$

$$= D_{KL}(\pi_{a|s}^D, \pi_{a|s}^U) + D_{KL}(\rho_s^D, \rho_s^U) \quad (60)$$

$$\geq D_{KL}(\pi_{a|s}^D, \pi_{a|s}^U) \quad (61)$$

$$= \sum_{s' \in \bar{S}} \rho^D(s) D_{KL}(\pi_{a|s=s'}^D, \pi_{a|s=s'}^U) \quad (62)$$

$$\geq \nu \sum_{s' \in \bar{S}} D_{KL}(\pi_{a|s=s'}^D, \pi_{a|s=s'}^U) \quad (63)$$

$$\geq \nu \sum_{s' \in \bar{S}} \frac{1}{2} \|\pi_{a|s=s'}^D - \pi_{a|s=s'}^U\|_1^2 \quad (\text{Pinsker's inequality}) \quad (64)$$

$$\geq \nu \max_{s' \in \bar{S}} \frac{1}{2} \|\pi_{a|s=s'}^D - \pi_{a|s=s'}^U\|_1^2 \quad (65)$$

$$(66)$$

and therefore, when constraining the state space to \bar{S} , denoted $\cdot|_{\bar{S}}$

$$\|P_{a|s|_{\bar{S}}}^D - P_{a|s|_{\bar{S}}}^U\|_1 = \|\pi_{a|s|_{\bar{S}}}^D - \pi_{a|s|_{\bar{S}}}^U\|_1 = \max_{s' \in \bar{S}} \|\pi_{a|s=s'}^D - \pi_{a|s=s'}^U\|_{TV} \leq \sqrt{2 \frac{\varepsilon}{\nu}}. \quad (67)$$

Note that this also implies the same bound for the test-time-constrained imitator, i.e.,

$$\|P_{a|s|_{\bar{S}}}^D - P_{a|s|_{\bar{S}}}^O\|_1 \leq \sqrt{2 \frac{\varepsilon}{\nu}}. \quad (68)$$

This is because only the deviating mass between D and U that lies on actions where D does not have support can be redistributed by the safety layer (because we assumed that D is safe, and hence those actions are safe and are not affected by adding a safety layer). But this deviation mass already lies where it has the maximum effect on the norm (namely: where D does not have any mass at all). So redistributing it will make the deviation not bigger.

Furthermore we have, just by the definition of the conditional probability matrix $P_{s,a|s}$

$$\|(P_{s,a|s}^O - P_{s,a|s}^D)\|_1 = \|(P_{a|s}^O - P_{a|s}^D)\|_1. \quad (69)$$

and the same holds when restricting the state to any subset, in particular \bar{S} .

Now, to finalize our argument to also bound the second term in Eq. (55), observe

$$\|(P_{s'|s}^O - P_{s'|s}^D) P_{s|s}^D\|_1 \quad (70)$$

$$= \|(P_{s'|s|_{\bar{S}}}^O - P_{s'|s|_{\bar{S}}}^D) P_{s|s|_{\bar{S}}}^D\|_1 \quad (\text{since } \bar{S} \text{ is the demonstrator support}) \quad (71)$$

$$\leq \|(P_{s'|s|_{\bar{S}}}^O - P_{s'|s|_{\bar{S}}}^D)\|_1 \|P_{s|s|_{\bar{S}}}^D\|_1 \quad (72)$$

$$= \|P_{s'|s,a}^O (P_{s,a|s|_{\bar{S}}}^O - P_{s,a|s|_{\bar{S}}}^D)\|_1 \|P_{s|s|_{\bar{S}}}^D\|_1 \quad (73)$$

$$\leq \|P_{s'|s,a}\|_1 \|P_{s,a|s|_{\bar{S}}}^O - P_{s,a|s|_{\bar{S}}}^D\|_1 \|P_{s|s|_{\bar{S}}}^D\|_1 \quad (74)$$

$$= \|P_{s'|s,a}\|_1 \|P_{a|s|_{\bar{S}}}^O - P_{a|s|_{\bar{S}}}^D\|_1 \|P_{s|s|_{\bar{S}}}^D\|_1 \quad (\text{Eq. (69)}) \quad (75)$$

$$\leq 1 \cdot \sqrt{2 \frac{\varepsilon}{\nu}} \cdot 1 \quad (\text{Eq. (68), 1-norm of stochastic matrix/vector is 1}). \quad (76)$$

³²The KL divergence is well-defined since we assumed that whenever the demonstrator has support, the imitator has also.

Coming towards the end, observe that plugging Eq. (55), (57) and (76) together gives

$$\Delta_{t+1} - \Delta_t \leq \sqrt{2 \frac{\varepsilon}{\nu}}$$

Therefore

$$\Delta_t = \sum_{t' \leq t} \Delta_{t'+1} - \Delta_{t'} \leq t \sqrt{2 \frac{\varepsilon}{\nu}}.$$

Then (keep in mind that we assumed that the reward depends only on the state)

$$|v^O - v^D| = \left| \sum_t (P_{s_t}^O - P_{s_t}^D) \cdot \vec{c} \right| \quad (77)$$

$$\leq \sum_t \| (P_{s_t}^O - P_{s_t}^D) \|_1 \| \vec{c} \|_\infty \quad (78)$$

$$= \| \vec{c} \|_\infty \sum_t \Delta_t \quad (79)$$

$$= \| \vec{c} \|_\infty \sum_t t \sqrt{2 \frac{\varepsilon}{\nu}} \quad (80)$$

$$\leq \| \vec{c} \|_\infty \sqrt{2 \frac{\varepsilon}{\nu} T^2}. \quad (81)$$

□

Note that if $\varepsilon > \frac{1}{T}$, then $\varepsilon T > 1$, but the maximum deviation cannot be larger than $T \|c\|_\infty < \varepsilon T T \|c\|_\infty$.

B. Further details

In this section, we gather further details as well as some additional results for several sections of the main part.

B.1. Further details on existence of differentiable injective – or any – safety layers (elaboration of Sec. 3.1)

An elaboration of the drawbacks of trying to construct safety layers solely based on diffeomorphisms:

Assume we are given a safe action set $\bar{A} \subset A$ (details follow in Sec. 3.2). We want to constrain our pre-safe generative policies pre-safe output $\hat{a} \in A$ into \bar{A} , without losing the property of having an exact density. To this end, first note that, theoretically, injective (for the change of variables) differentiable mappings into \bar{A} can in principle exist: for instance, the *Riemann mapping theorem* (Lutcher, 2010) tells us that such a mapping exists from \mathbb{R}^2 to \bar{A} , if \bar{A} is a simply connected³³ open set in \mathbb{R}^2 .

However, along this line, there are several limitations:

First, as soon as \bar{A} is not simply connected (while A is), topology directly tells that there cannot be a differentiable injection.

Second, injectivity can be a very strong requirement when constructing functions.³⁴

Third, e.g., often Riemann mappings are rigid and just exist implicitly as a solution to some variational or partial differential equation problem.

³³An open set in \mathbb{R}^n is called *(path-)connected*, if any two of its elements can be connected by a continuous path within the set; and *simply connected* if these connecting paths are, up to continuous deformations within the set, unique.

³⁴An intuitive reason why we need injectivity for the change of variables formula is that we need to know the pre-image of infinitesimal hypercube volume elements, with which the original density $p_{\hat{a}}$ is multiplied for the original probability, in order to rescale the density $p_{\hat{a}}(g^{-1}(a))$ for the measure after g .

B.2. Further details/remarks on the safe set inference, safe control, etc. (Sec. 3.2)

Regarding inner approximations of the safe set For as little as possible bias and conservativity, we need the inner approximation of the safe set to be as large as possible. In principle, one could also just give a finite set of points as inner approximation, but this could be very unflexible and biased, and injectivity for change-of-variables Prop. 1 would not be possible.

Regarding safety between discrete time steps Note that our setup is discrete time, but it can directly also imply safety guarantees between time stages: e.g., for our experiments, we know maximum velocity of the agents, so we know how much they can move at most between time stages, and we can add this as a margin to the distance-based safety cost.

Primitive fallback maneuvers Regarding the ego, note that the search over a small set of future trajectories in the form of the “*fallback maneuvers*” (instead of an exhaustive search/optimization over the full planning/trajecotry space) can be seen as a simple form of motion primitives or graph search methods and related to “sampling-based” planning approaches (Paden et al., 2016). Regarding the others, considering only a small subset of possible behaviors (which, of course, weakens guarantees but is at least a tractable way) is also somewhat related to sampling-based methods in continuous game theory (Adam et al., 2021) as well as empirical/oracle-based game theory (Lanctot et al., 2017). Note: Here we assume separability of the state between ego and others.

B.3. Further details on GAIL loss and training (Sec. 3.3)

B.3.1. IMITATION LOSS

Let us elaborate on the GAIL-based (Ho & Ermon, 2016) cost function. We do it more generally here to also include Wasserstein-GAIL/GAN. The reason why we consider using the Wasserstein-version (Xiao et al., 2019) is the following: Due to safety constraints, if the demonstrator is unsafe, we may deal with distributions of disjoint support. Then we want to encourage “geometric closeness” of distributions. But this is not possible with geometry-agnostic information-theoretic distance measures.

To specify the imitation cost c that we left abstract in Sec. 2 and 3.3, let

$$c(s, a) = e_2(s, a), \quad (82)$$

$$(e_1, e_2) = \arg \max \mathbb{E}_{\pi^D} \left(\sum_t e_1(s_t, a_t) \right) \quad (83)$$

where the arg max ranges over pairs (e_1, e_2) of bounded functions from some underlying space of bounded functions (Xiao et al., 2019): besides Eq. (83), the following is required (Xiao et al., 2019):

$$e_1(x) + e_2(y) \leq \delta(x, y), \quad (84)$$

for some underlying distance δ . This condition is referred to as *Lipschitz regularity*. e_1, e_2 are called *Kantorovich potentials*.

As classic example (which we use as default in the main part), when taking $e_1(s, a) := \log(1 - D(s, a))$ and $e_2(s, a) := \log(D(s, a))$, for some function D , then this exactly amounts to the classic GAN/GAIL formulation with discriminator D .

B.3.2. TRAINING

Regarding the policy optimization step (b) sketched in Sec. 3.3, note that: For each sampled state s_t , $\pi^{I, \theta}(a|s_t)$ implicitly remembers the safe set \hat{A}_t^s , such that also after any policy gradient step its mass will always remain within the safe set. Note that for this to work, it can be a problem if at some point we took a safe fallback action (Sec. 3.2) and thus only know a *singleton* safe set (and it is not a function of current state only). Since this is rare, it should pose little problems to training. Rigorously addressing this is left to future work.

B.4. Further experimental and architecture details

Remark: Code will be made available upon publication.

We conjecture that a guarantee can be given for the l_∞ setting even without convexity over all dimensions, simply by the l_∞ norm being a minimum over dimensions and then in some way considering each dimension individually.

As Gaussian policy, we take two hidden layers each 1024 units, using leaky ReLUs as non-linearities. (As conditional flow policy, we experimented with a conditional flow with two hidden layers a 128 units.) As discriminator, we take a NN with two hidden layers and 48 units each.

The data set (scene) consists of ~ 1500 tracks (trajectories), of which we use 300 as test set and 100 as validation, and the rest as training set.

One full safe set computation with some limited vectorized parts takes around 1.5s on a standard CPU. We believe vectorizing/parallelizing more of the code can further reduce this substantially.

C. Further related work

More broadly related is also the following work:

Certain safety layers (Donti et al., 2021; Dalal et al., 2018) are a special case of so-called *implicit layers* (Amos & Kolter, 2017; Amos et al., 2018; El Ghaoui et al., 2019; Bai et al., 2019; Ling et al., 2018; 2019), which have recently been applied also for game-theoretic multi-agent trajectory model learning (Geiger & Straehle, 2021), including highway driver modeling; robust learning updates in deep RL (Otto et al., 2021); and learning interventions that optimize certain equilibria in complex systems (Besserve & Schölkopf, 2021).

Boborzi et al. (2021) similar to us propose a safe version of GAIL, but there are several differences: they build on a different safety reasoning (RSS), which is specific for the scope of driving tasks, while our full method with its worst-case safety reasoning is applicable to general IL domains, and they do not provide exact densities/gradients of the full safe policy as we do.

Worth mentioning is also work on safe IL that builds on hierarchical/hybrid approaches that combine imitation learning with classic safe planning/trajectory tracking (Chen et al., 2019; Huang et al., 2019).